IMPACT STUDIES WITH PERIDYNAMICS

Carlos J. Ruestes[a], Diego R. Tramontina[a] and Eduardo M. Bringa[a,b]

[a]*Instituto de Ciencias Básicas, Universidad Nacional de Cuyo, Parque Gral. San Martín,
5500 Mendoza, Argentina, cjruestes@gmail.com, diego.tramontina@gmail.com, ebringa@yahoo.com,
https://sites.google.com/site/simafweb/home*

[b]*CONICET, 5500 Mendoza, Argentina*

Keywords: Peridynamics, Fragmentation, Impact, Cluster collisions.

Abstract. Several impact and fragmentation scenarios were studied using peridynamics, including impact on thin discs, taking into consideration the stiffness of the impactors and its influence on the fragmentation pattern. The promising peridynamics theory allows bypassing the mathematical singularity that a fracture represents within the classical theory of continuum mechanics, conditioned to the constitutive models available for such a problem. In our tests, the prototype microelastic brittle model was used, and the influence of the constitutive model parameters on discs and spheres fragmentation was studied. Collision and fragmentation of spherical clusters are compared to similar results using atomistic and granular models.

1 INTRODUCTION

A complex problem of great importance for solid mechanics is related to the formation of discontinuities in a region where they do not initially exist. Typical cases include failure of mechanical components due to cracking and / or fracture as a result of dynamic loads, high thermal gradients, impact, explosions, etc. Mechanical and structural design is usually based on continuum mechanics (Malvern, 1969), and the mathematical framework developed for this theory is based on partial derivatives to represent the relative displacements and forces between neighboring elements. By definition, partial derivatives with respect to spatial coordinates are not defined in the discontinuities of the bodies and, for this reason, the classical approach of continuum mechanics is not well suited for the modeling of problems such as the ones mentioned before. To overcome this issue, various techniques have been implemented with relative success. For instance, in the case of the cohesive finite element method (Camacho and Ortiz, 1997; Xu and Needleman, 1996), cracks can only follow the path where the cohesive zone elements are placed, which means that the actual crack path is severely constrained. As an alternative, the extended finite element method (Belytschko et al., 2009) is enriched with functions for an approximation where a discontinuous displacement field exists, allowing a crack to pass through the elements rather than along the element boundaries. However, this might not be a suitable option for problems where more than a couple of cracks develop in the sample, as in most fragmentation studies. These approximations limit, at least partially, the usefulness of these techniques in cases where no discontinuity exists initially and gets formed after mesh generation and application of the loading state to be simulated.

In an attempt to overcome the problem introduced by the classical mathematical formulations, a new theory called peridynamics (Silling, 2000) was formulated. Its essence is the use of integral equations to compute the force over a non-local region around each point, thus replacing the divergence of the stress tensor in the equations of motion, and since spatial derivatives are not used, peridynamic equations remain valid at points or surfaces of discontinuity, such as a crack.

2 BASIC FORMULATION

The non-local formulation described above was named peridynamics after the greek root "peri", which means "near". In peridynamics, every point of the material is connected through bonds to all points inside a certain region limited by a horizon δ. Then an integral equation is used to compute the current point forces per unit volume. Spatial differentiation is not used, so this methodology can be applied over discontinuous displacement fields. Unlike classical continuum theory, in peridynamics theory, during the initial configuration, each point gets linked directly not only to their immediate neighbors, but also with every particle that is located within the horizon of interaction δ. For this reason, this method is described as non-local. The peridynamic equation of motion is given by equation (1).

$$\rho \ddot{\boldsymbol{u}}(\boldsymbol{x}, t) = \int_H \boldsymbol{f}(\boldsymbol{u}(\boldsymbol{x'}, t) - \boldsymbol{u}(\boldsymbol{x}, t), \boldsymbol{x'} - \boldsymbol{x}) dV_{\boldsymbol{x'}} + \boldsymbol{b}(\boldsymbol{x}, t) \tag{1}$$

Where $\boldsymbol{b}$ represents the external force per unit volume, $\boldsymbol{f}$ is the pairwise force function in the bond that connects point $\boldsymbol{x}$ and $\boldsymbol{x}$', and contains all the constitutive information of the material. $\boldsymbol{u}$ is the displacement vector field and ρ is the density of the material. The integral term results in the force per unit reference volume squared due to interaction with other points.

Lets define $\boldsymbol{\xi}$, relative position vector in the initial configuration as

$$\boldsymbol{\xi} = \boldsymbol{x}' - \boldsymbol{x} \tag{2}$$

and a relative displacement vector $\boldsymbol{\eta}$ as

$$\boldsymbol{\eta} = \boldsymbol{u}' - \boldsymbol{u} \tag{3}$$
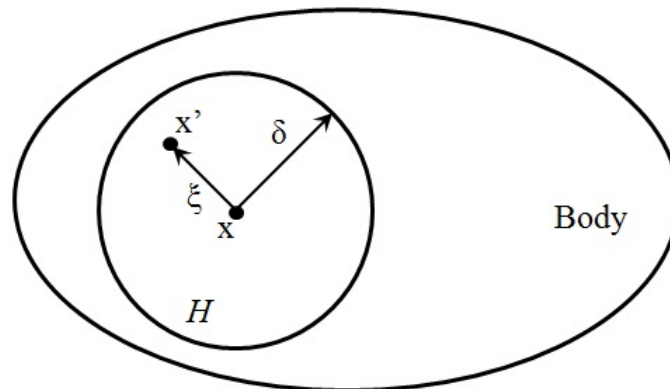
Figure 1: Each point $\boldsymbol{x}$ in the body interacts directly with all of its neighboring points inside the sphere H of radius δ.

Note that $\boldsymbol{\eta} + \boldsymbol{\xi}$ represents the current relative position vector between the points.

The $\boldsymbol{f}$ function must comply with the following properties:

$$\boldsymbol{f}(-\boldsymbol{\eta}, -\boldsymbol{\xi}) = -\boldsymbol{f}(\boldsymbol{\eta}, \boldsymbol{\xi}) \qquad \forall \; \boldsymbol{\eta}, \boldsymbol{\xi} \tag{4a}$$

$$(\boldsymbol{\xi} + \boldsymbol{\eta}) \times \boldsymbol{f}(\boldsymbol{\eta}, \boldsymbol{\xi}) = 0 \qquad \forall \; \boldsymbol{\eta}, \boldsymbol{\xi} \tag{4b}$$

Equation (4a) ensures conservation of linear momentum while Eq.(4b) ensures conservation of angular momentum.

Since is not the objective of this work to provide a formal and complete presentation of peridynamic theory, we omit the remaining proofs, which were developed by Silling (2000) with subsequent generalization in Silling and Askari (2005) and Silling et al. (2007). However, it is important to note that this theory and its formulation, as presented here, implies the following limitations:

Isotropy: The response of the material is independent of orientation. For anisotropic materials, such as multilayered composites, the dependency on the binding energy with respect to the orientation can be made explicit by means of a suitable definition of a directional potential associated to the function f.

Elasticity: In the simple case of a purely elastic material, each pair of particles $\boldsymbol{x}$ and $\boldsymbol{x}$' are connected by a spring, but it is also possible to include non-linear characteristics to this formulation. The elasticity defined at the micro level, brings with it the definition of an elasticity at the macro level through a macroelastic energy density, analogous to the conventional strain energy defined in the classical theory for an elastic solid.

Harmonic Material: an isotropic and microelastic material defined as in this theory, it is called harmonic, since any displacement field satisfies the Laplace equation.

3   THE PMB MODEL

The case studies developed in this work were developed using LAMMPS (Plimpton, 1995), an open source code where the peridynamic theory is implemented in its bond-based formulation (Parks et al., 2008). The constitutive model used in this study is referred to as PMB, (prototype microelastic brittle), a prototype of a brittle material where the pairwise forces derive from a scalar micro-potential. This model was developed from the model of a microelastic and isotropic material, where the bond strength depends only on the bond stretching (spring) through equation (5).

$$s = \frac{|\boldsymbol{\xi} + \boldsymbol{\eta}| - |\boldsymbol{\xi}|}{|\boldsymbol{\xi}|} = \frac{y - |\boldsymbol{\xi}|}{|\boldsymbol{\xi}|} \tag{5}$$

Failure can be introduced into the model by allowing the bonds to be broken when they are stretched beyond a certain limit. After breakage, the bond is unable to bear loading and will remain broken from that moment on, i.e. there is no possibility that the link will recover.

The PMB material is defined by the following expressions,

$$f(y(t), \boldsymbol{\xi}) = g(s(t, \boldsymbol{\xi})) \, \mu(t, \boldsymbol{\xi}), \tag{6a}$$

$$g(s) = cs \quad \forall s, \tag{6b}$$

$$\mu(t, \boldsymbol{\xi}) = \begin{cases} 1, & \text{if } s(t', \boldsymbol{\xi}) < s_0 \quad \text{for} \quad 0 \le t' \le t \\ 0, & \text{otherwise} \end{cases} \tag{6c}$$

Where c is the spring constant, and s_0 is the critical bond stretch. As shown above, the pairwise force function (Eq. 6a) is the product of a linear function carrying the elastic characteristic of the bond (Eq. 6b) with a scalar valued function that fixes the stretching limit and also ensures history dependence (Eq. 6c), in other words, that the bond will remain failed after breaking. For simplicity we will assume that both c and s_0 are constant and defined by the following expressions,

$$c = \frac{18k}{\pi \delta^4} \tag{7}$$

$$s_0 = \sqrt{\frac{10G_0}{\pi c \delta^5}} = \sqrt{\frac{5G_0}{9k\delta}} \tag{8}$$

Where k is the bulk modulus of the material and G_0 is the work required to break all bonds per unit fracture area. As it can be seen, both the spring constant and the critical bond stretch depend not only on properties of the material but also on the chosen horizon, δ. A complete review on the use of the peridynamic horizon δ and its implications on crack branching of brittle materials is available in Bobaru and Hu (2012). This formulation is an oversimplification because it assumes that the critical bond length is independent of the conditions in the surrounding bonds. As suggested in the literature (Silling and Askari, 2005), in case of brittle materials like glass, this situation can be dealt with the help of the following definition

$$s_0(t) = s_{00} - \alpha s_{\min}(t) \tag{9a}$$

$$s_{\min}(t) = \min_{\boldsymbol{\xi}} \left\{ \frac{y(t) - |\boldsymbol{\xi}|}{\boldsymbol{\xi}} \right\} \tag{9b}$$

Where $s_{\min}$ is the current minimum stretch among all bonds connected to a given point, and where s_{00} and α are constants, with α typically about 1/4. Finally, a short-range repulsive force is available in the LAMMPS module to avoid overlapping of particles that are released after the breakage of all their bonds (Parks et al., 2008).
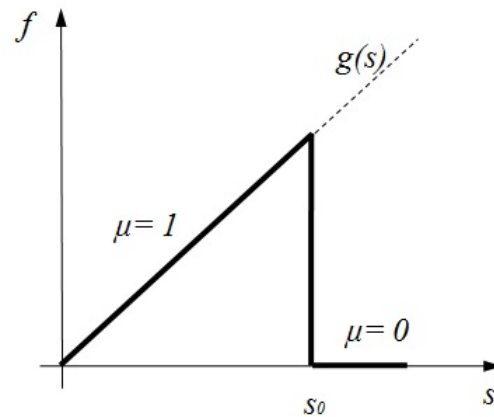
Figure 2: Bond force as a function of the stretching in the PMB model. As shown in Eq.6c, μ is a scalar valued function which carries the history dependence. Once μ reaches zero, it remains unchanged for the rest of the simulation.

LAMMPS peridynamics implementation keeps track of the damaged sustained by the particles through a per-atom vector whose modulus ranges from zero (no damage) to one, the latter indicating that the particle is no longer linked with its neighbors. Implementation details are available at the software website (lammps.sandia.gov).

4 CASE STUDIES

4.1 Impact on a plate

A case widely discussed in the available literature (Silling and Askari, 2005; Parks et al., 2008) is the impact of a spherical rigid indenter of 5 mm radius on a plate of 74 mm diameter and 2.5 mm thick, simulated with the LAMMPS PMB model with constants $c = 1.6863 \ e + 22$, $s_{00} = 0.0005$ and $\alpha = 0.25$, using a density of 2000 kg/m^3 and a volume per particle of $1.25 \ e - 10$ m^3. These values are typical of a glass-like material with a bulk modulus of 14.9 GPa and $G_0 = 10$ J/m^2. The impact velocity of the indenter is set at 100 m/s. In order to get closer to the representation of a real material with its imperfections, and to avoid perfectly symmetric patterns in the structure of the sample, a random displacement of the order of 0.005 mm was introduced into the initial position of each particle. This slight disturbance, a thousand times smaller than the lattice parameter, was enough to decrease the number of links generated in the sample by 10 percent.

After successful reproduction of the results shown in the references (Parks et al., 2008) for a rigid indenter (Fig.3a), we considered the effect of the stiffness of the projectile in the fragmentation pattern of the sample. To this end, we proceeded to replace the rigid indenter by a sphere of the same material as the target, maintaining all the dimensions, parameters and conditions of

(a)   (b)
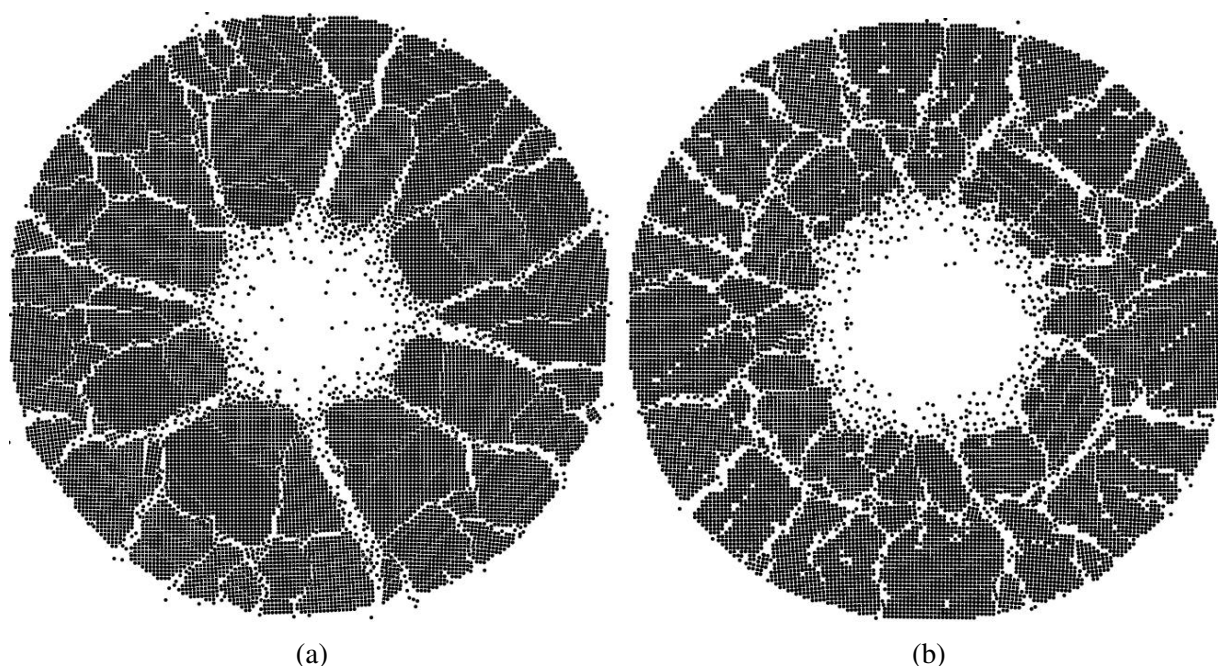
Figure 3: Fragmentation pattern for a simulation considering (a) rigid indenter, and (b) a non-rigid indenter. The fracture pattern clearly exhibits the expected radial and hoop cracks for both cases, although radial cracks are more noticeable than hoop cracks for the rigid indenter case. Very good agreement is found when compared to experimental results (Bouzid et al., 2001).

the previous simulation. Simulation time was extended to 8 ms to obtain a clear fracture pattern, shown in Fig.3b.

Quantitatively, damage was tracked by means of a computation of damage per particle, as explained above, with a normalization against the total number of particles belonging to the plate. This calculation revealed a normalized damage of 0.23 for the plate indented by the non-rigid projectile against a damage of 0.17 for the rigid indenter, a 35% increase in the case of a non-rigid indenter. These values correspond to particles that reached damage equal to one, i.e. complete damage (disconnection from other particles). The possibility of the indenter to collapse during impact increases the hit area in the plate, leading to momentum transfer over a wider area, which is the reason why the hole produced in the center of the plate together with the area of fractured debris is larger for the sample hit by the non-rigid indenter. While radial cracks are more important that hoop cracks in the rigid indenter case, this contrast is not seen for the non-rigid indenter example.

4.2   Cluster-cluster impact

Another case of potential application is the study of cluster collisions in astrophysics. These problems are typically beyond the scope of continuum-type models when scale goes down to micrometers or below. Since this type of collisions can occur between porous and non-porous brittle solids, a peridynamics PMB model approach might be useful in such cases, provided plastic effects are negligible and phase changes do not occur.

As a test case, the collision of two spherical clusters with a non-zero impact parameter was simulated.

Each cluster was considered as a sphere of 280 micrometer radius containing 33460 spher-
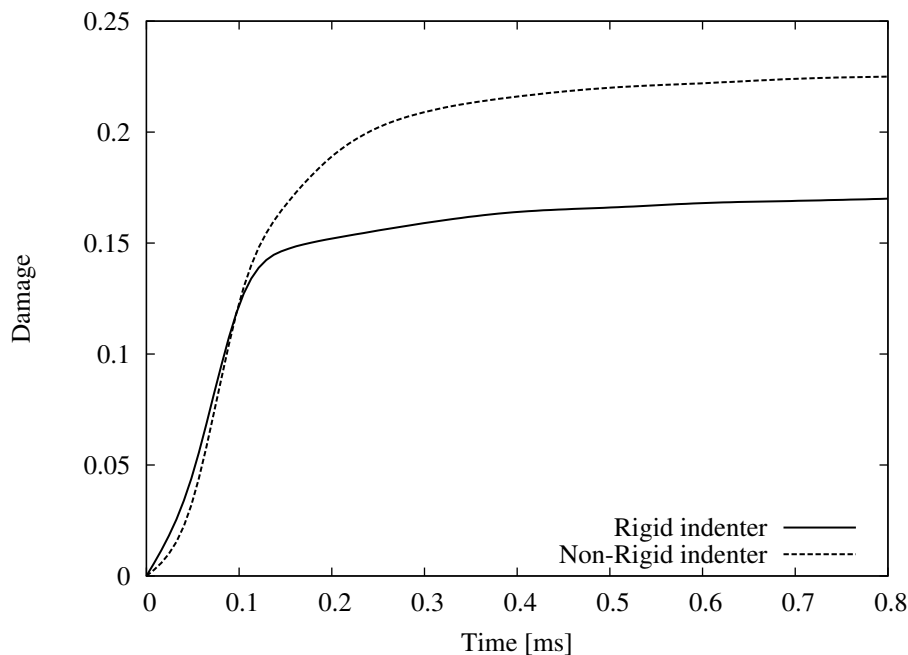
Figure 4: Damage evolution for the indented plate simulation. Up to 0.1 ms, the rigid indenter transfers energy more effectively than the non-rigid one, since the latter consumes part of its initial energy in its own fragmentation. However, after 0.1 ms, this fragmentation allows for a more effective energy transfer to the plate, explaining the 35 % increment in damage with respect to the rigid indenter case.

ical grains of 7 micrometer radius each. The PMB model was configured with constants $c = 1.1317 \ e + 23$, $s_{00} = 0.0023$ and $\alpha = 0.25$, using a density of 2000 kg/m^3 and a volume per particle of $1.44 \ e - 15$ m^3. These values correspond to a material with a fragmentation velocity close to 0.15 m/s. This quantity is important in cluster collision fragmentation studies and is defined as the smallest velocity that, when imparted to a bounded pair of grains, produces its dissociation. In this case, the chosen value is of the order of the value reported by Ringl et al. (2012) for their silica grains simulations. The collision was set at a relative speed of 5 m/s with an impact parameter equal to the cluster radius.

Damage was tracked and normalized in the same manner as described in the preceding section. Its evolution is shown in Fig.6 and allows us to conclude that the fragmentation and evaporation seen in Fig.5 is mainly produced between frames (b) and (g) of Fig.5, i.e. between 0.05 and 0.3 ms. This fragmentation and evaporation of single grains also occurs in Ringl et al. (2012) for their granular model simulations. This behavior is also in good qualitative agreement with MD atomic cluster collisions as studied by Kalweit and Drikakis (2006) for nanoscale clusters, and it can be seen that, as expected for the initial velocity of the clusters, fragmentation occurs instead of sticking. Significant scattering is also visible and a torque effect is present due to the non-zero impact parameter chosen for our simulations.

(a) 0.0 ms

(b) 0.05 ms

(c) 0.1 ms

(d) 0.15 ms

(e) 0.2 ms

(f) 0.25 ms

(g) 0.3 ms

(h) 0.35 ms
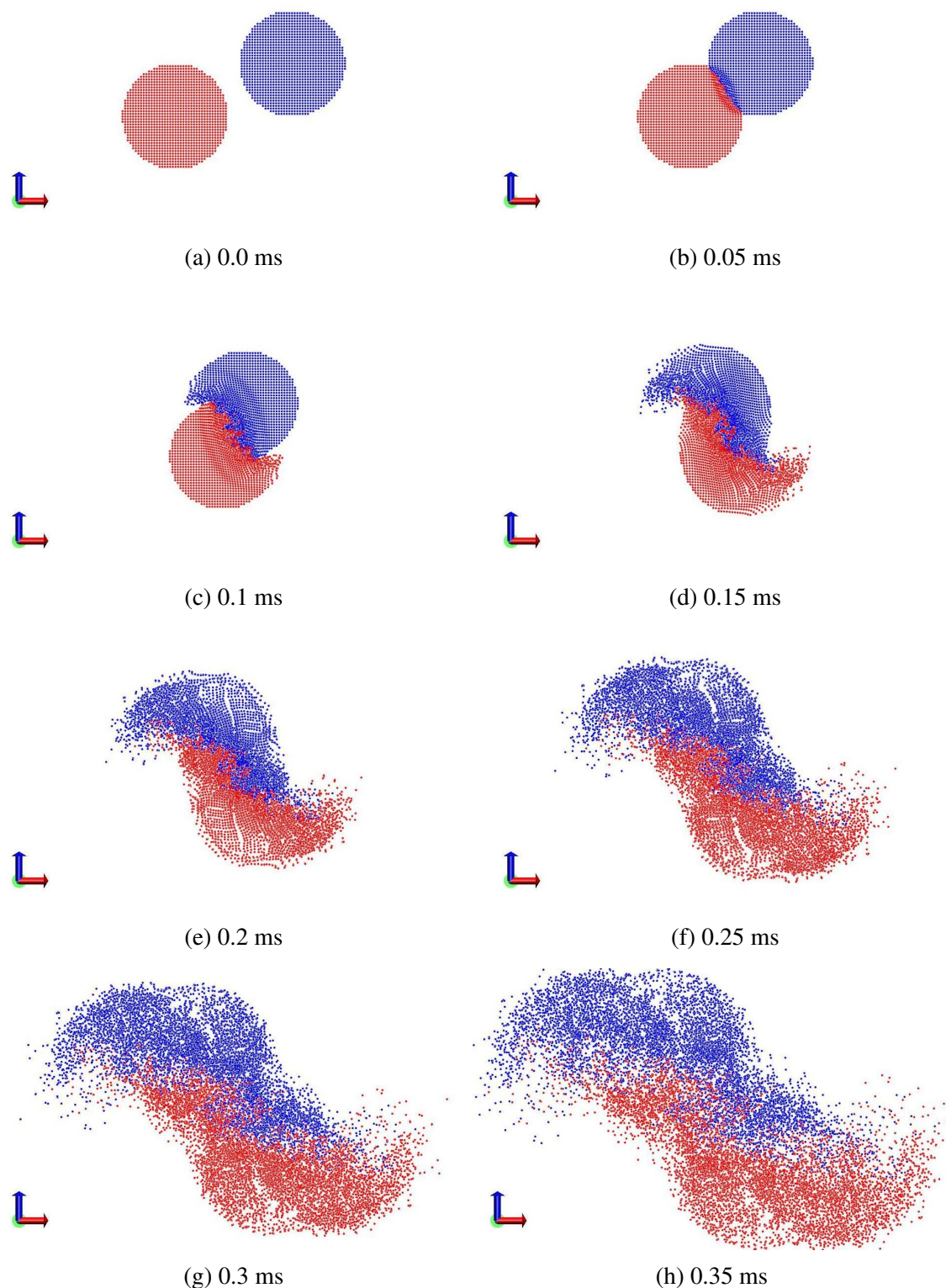
Figure 5: Cluster impact evolution. After colliding, the grains in the contact zone get compacted and dragged by the material of the other cluster, widening the contact area and causing extensive deformation. A large quantity of grains are scattered in the process, mainly in the contact area. It is also possible to see chains of grains detaching from the superficial layers. Starting at 0.15 ms and continuing at 0.2 ms, cracks are generated, which contribute to the destruction of the cluster structure, increasing the number of free particles. The collision continues with a catastrophic destruction where the clusters are completely evaporated into single grains. No difference exists in the composition or characteristics of the clusters as the colors are used for differentiation purposes only.
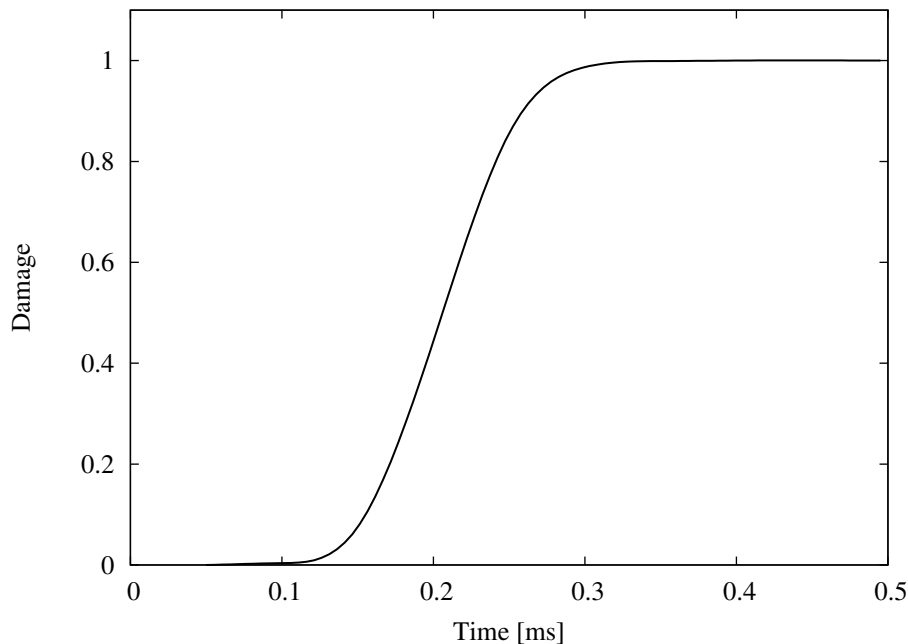
Figure 6: Damage evolution for the cluster-cluster collision simulation. Between 0.05 ms and 0.1 ms, contact between spheres occurs, and the fragmentation process lasts for the following 0.2 ms. During this time, direct contact between clusters and wave propagation in each cluster contribute to damage evolution. Clusters are completely fragmented into single grains 0.3 ms after contact begins.

5 CONCLUSIONS AND FUTURE WORK

We presented an introduction to peridynamics theory, and a constitutive model, PMB (prototype microelastic brittle), adequate for our case studies. Starting from the successful reproduction of an example available in the literature (Parks et al., 2008), a simulation was performed for a collapsible projectile, verifying its influence on the fragmentation pattern, as compared to a rigid projectile. Good agreement in the fragmentation pattern was obtained against experimental results (Bouzid et al., 2001). Damage tracking was used to monitor damage evolution, showing that, although a rigid indenter produces more damage during the early stages of the impact simulation, the collapse of the non-rigid indenter allows for a higher energy transfer, producing 35 % more damage at the end of the simulation.

The peridynamics PMB model was also applied to cluster-cluster impact studies in the fragmentation regime, with good agreement against granular and atomistic models (Ringl et al., 2012). The peridynamics simulation was able to capture the process of cracking and subsequent fragmentation up to catastrophic breaking of the clusters. Since sticking is not contemplated into the constitutive model, no tests were performed in the agglomeration/sticking regime. While this simulation can certainly be improved with proper adjustment, not only of the model parameters but also of the model itself, e.g. enabling agglomeration and compaction, they clearly show the potential of peridynamic theory for this kind of applications, and efforts are already being directed in order to treat granular materials with peridynamics in other fields (Lammi and

Vogler, 2012).

Significant efforts can be found to extend the scope of peridynamic theory to other case studies and materials (Ha and Bobaru, 2010; Silling and Bobaru, 2005; Askari et al., 2006). A major development of constitutive models, would increase the number of multiscale applications of the theory, including constitutive models which can be developed through studies with the help of atomistic studies and then applied to classical problems of continuum mechanics coupled with peridynamics (Macek and Silling, 2007).

We plan to apply the model presented here to study porous brittle materials, while continue exploring the large parameter space for impact simulations with astrophysical significance.

6 ACKNOWLEDGEMENTS

REFERENCES

Askari E., Xu J., and Silling S. Peridynamic analysis of damage and failure in composites. In *In 44th AIAA Aerospace Sciences Meeting and Exhibit*. 2006.

Belytschko T., Gracie R., and Ventura G. A review of extended/generalized finite element methods for material modeling. *Modelling and Simulation in Materials Science and Engineering*, 17(4):043001, 2009. ISSN 0965-0393, 1361-651X. doi:10.1088/0965-0393/17/4/043001.

Bobaru F. and Hu W. The meaning, selection, and use of the peridynamic horizon and its relation to crack branching in brittle materials. *International Journal of Fracture*, 176(2):215–222, 2012. ISSN 0376-9429, 1573-2673. doi:10.1007/s10704-012-9725-z.

Bouzid S., Nyoungue A., Azari Z., Bouaouadja N., and Pluvinage G. Fracture criterion for glass under impact loading. *International Journal of Impact Engineering*, 25(9):831–845, 2001. ISSN 0734743X. doi:10.1016/S0734-743X(01)00023-9.

Camacho G. and Ortiz M. Adaptive lagrangian modelling of ballistic penetration of metallic targets. *Computer Methods in Applied Mechanics and Engineering*, 142(3-4):269–301, 1997. ISSN 00457825. doi:10.1016/S0045-7825(96)01134-6.

Ha Y.D. and Bobaru F. Studies of dynamic crack propagation and crack branching with peridynamics. *International Journal of Fracture*, 162(1-2):229–244, 2010. ISSN 0376-9429, 1573-2673. doi:10.1007/s10704-010-9442-4.

Kalweit M. and Drikakis D. Collision dynamics of nanoscale lennard-jones clusters. *Physical Review B*, 74(23), 2006. ISSN 1098-0121, 1550-235X. doi:10.1103/PhysRevB.74.235415.

Lammi C.J. and Vogler T.J. Mesoscale simulations of granular materials with peridynamics. pages 1467–1470. 2012. doi:10.1063/1.3686559.

Macek R.W. and Silling S.A. Peridynamics via finite element analysis. *Finite Elements in Analysis and Design*, 43(15):1169–1178, 2007. ISSN 0168874X. doi:10.1016/j.finel.2007.08.012.

Malvern L. *Introduction to the Mechanics of a Continuous Medium*. Prentice-Hall, Inc., Englewood Cliffs, New Jersey, USA, 1969. ISBN 13-487603-2.

Parks M.L., Lehoucq R.B., Plimpton S.J., and Silling S.A. Implementing peridynamics within a molecular dynamics code. *Computer Physics Communications*, 179(11):777–783, 2008. ISSN 00104655. doi:10.1016/j.cpc.2008.06.011.

Plimpton S. Fast parallel algorithms for short-range molecular dynamics. *Journal of Computational Physics*, 117(1):1–19, 1995. ISSN 00219991. doi:10.1006/jcph.1995.1039.

Ringl C., Bringa E.M., Bertoldi D.S., and Urbassek H.M. Collisions of porous clustes: a granular-mechanics study of compaction and fragmentation. *The Astrophysical Journal*, 752(2):151, 2012. ISSN 0004-637X, 1538-4357. doi:10.1088/0004-637X/752/2/151.

Silling S. Reformulation of elasticity theory for discontinuities and long-range forces. *Journal of the Mechanics and Physics of Solids*, 48(1):175–209, 2000. ISSN 00225096. doi:10.1016/S0022-5096(99)00029-0.

Silling S. and Askari E. A meshfree method based on the peridynamic model of solid mechanics. *Computers & Structures*, 83(17-18):1526–1535, 2005. ISSN 00457949. doi:10.1016/j.compstruc.2004.11.026.

Silling S. and Bobaru F. Peridynamic modeling of membranes and fibers. *International Journal of Non-Linear Mechanics*, 40(2âĂŞ3):395 – 409, 2005. ISSN 0020-7462. doi:10.1016/j.ijnonlinmec.2004.08.004. <ce:title>Special Issue in Honour of C.O. Horgan</ce:title>.

Silling S.A., Epton M., Weckner O., Xu J., and Askari E. Peridynamic states and constitutive modeling. *Journal of Elasticity*, 88(2):151–184, 2007. ISSN 0374-3535, 1573-2681. doi:10.1007/s10659-007-9125-1.

Xu X.P. and Needleman A. Numerical simulations of dynamic crack growth along an interface. *International Journal of Fracture*, 74(4):289–324, 1996. ISSN 0376-9429, 1573-2673. doi:10.1007/BF00035845.